Catalysis Letters 61 (1999) 7–13

Prospects for detecting metal–adsorbate vibrations by sum-frequency spectroscopy

Christopher T. Williams [a], Yong Yang [a,b] and Colin D. Bain [a,*]

[a] *Physical and Theoretical Chemistry Laboratory, University of Oxford, South Parks Road, Oxford OX1 3QZ, UK*
[b] *State Key Laboratory for Physical Chemistry of Solid Surfaces and Institute for Physical Chemistry, Xiamen University, Xiamen, Fujian 361005, PR China*

Received 7 May 1999; accepted 8 June 1999

Sum-frequency spectroscopy (SFS) was used in an attempt to detect the platinum–carbon vibration of CO adsorbed on Pt(111). The international free-electron laser FELIX at the FOM Institute, Rijnhuizen, provided the required tunable far-infrared (19–23 μm) source, while complementary measurements in the C–O stretch region (4.7–5.1 μm) were performed at the University of Oxford with a conventional nanosecond laser system. Ordered Pt(111) surfaces were prepared by the H_2/O_2 flame annealing approach and CO monolayers were produced by exposure of the Pt crystal to gaseous CO in a flow reactor. The monolayers were characterized by sum-frequency (SF) measurements of the $\nu_{C–O}$ vibrational frequency. The CO adsorbed primarily in the terminal (atop) configuration, with a $\nu_{C–O}$ frequency of around 2078 cm^{-1}. In the far-IR region, the non-resonant background from the Pt substrate could readily be detected by SFS, but there was no evidence for the $\nu_{Pt–CO}$ mode. Direct laser-induced desorption and thermal desorption of CO are unlikely under the experimental conditions. It is therefore probable that the intrinsic cross-section of the Pt–CO mode is too low for easy detection by SFS. The implications for the use of SFS to detect metal–adsorbate vibrational modes are discussed in light of these findings.

Keywords: sum-frequency spectroscopy, Pt(111), carbon monoxide, adsorption, far-infrared, free-electron laser

1. Introduction

Monitoring the presence and behavior of adsorbed molecules on metal surfaces during heterogeneous catalytic reactions is of central importance for elucidating reaction mechanisms. Much progress has been made towards our understanding of the surface chemistry of metal-catalyzed reactions by the combination of ultra-high vacuum (UHV) experimental tactics with rate and selectivity measurements performed under more technologically relevant conditions (for a recent review see [1]). Nevertheless, there remains a general difficulty in extrapolating results obtained at the low pressures (and sometimes temperatures) used in UHV studies to reaction conditions encountered in industrial applications. As a result, increasing emphasis is being placed on the development of new experimental approaches that can be used to study surfaces under reaction conditions.

Sum-frequency spectroscopy (SFS) is a type of vibrational spectroscopy that has been used to examine a range of interfacial phenomena that are important in chemical and engineering science (for a recent review see [2]). SFS is based on the second-order non-linear optical effect of sum-frequency generation (*vide infra*), and is a selective probe of vibrational modes of interfacial molecules to the exclusion of bulk-phase interferences commonly encountered with other techniques. Furthermore, SFS can often provide quantitative information on interfacial molecular orientation. Over the past few years SFS has begun to be applied to problems in heterogeneous catalysis. Somorjai and co-workers used SFS to investigate CO oxidation [3] and alkene hydrogenation [4] and dehydrogenation [5] on Pt(111) single crystals over a range of pressures. Hirose and co-workers employed SFS to examine the interaction of NO and CO on Ni/NiO(100) [6] as well as formic acid adsorption on MgO(001) [7]. Tadjeddine and co-workers have examined the formation of adsorbed CO during electrochemical oxidation of methanol on platinum surfaces, a process important for fuel cell technology [2b].

SFS has proven useful for examining intramolecular vibrations of molecules adsorbed on both metal and metal oxide surfaces. The majority of such studies have been limited to vibrational modes between 1000 and 3500 cm^{-1} (ca. 3–10 μm), primarily because bench-top laser systems [8] do not generate sufficient infrared power for non-linear mixing experiments at wavelengths much greater than 10 μm. The development of free-electron lasers in recent years now allows the entire vibrational infrared (3–100 μm) to be covered by intense, broadly tunable sources. A few groups have begun to use these free-electron lasers to detect longer wavelength vibrations (>10 μm) with SFS (see, for example, [9]). Recently, Braun et al. demonstrated SFG from an Ag/thiophenol interface at wavelengths up to 54 μm using the free-electron laser FELIX at the FOM Institute, Rijnhuizen [10]. Both an in-plane ring deformation (14 μm, 700 cm^{-1}) and the C–S stretch (24 μm, 420 cm^{-1}) were observed, the longest wavelength molecular vibrations yet reported by SFS.

* To whom correspondence should be addressed.

The ability to probe metal–adsorbate vibrations, which, with the exception of hydrides, are usually located below ca. 700 cm^{-1}, would be invaluable for *in situ* studies of heterogeneous catalysis. The most widely used technique for detecting these vibrations, electron energy loss spectroscopy (EELS), is very powerful in UHV environments but is not applicable at elevated pressures. Only surface-enhanced Raman spectroscopy (SERS) has been successfully used to probe metal–adsorbate vibrations under catalytic reaction conditions (for examples see [11]). A clear need exists for general techniques that can access this spectroscopic region. Although recent results have shown that SFG from metal surfaces can readily be detected at these wavelengths, attempts to detect metal–adsorbate modes (in Ag/thiophenol and Pt(100)/sulfur) have so far proved unsuccessful [10]. However, metal–S vibrations may simply be too weak to observe with SFS. It therefore still remains to be demonstrated that SFS will be useful for examining metal–adsorbate vibrational modes.

In an effort to establish whether or not SFS will be widely useful for probing metal–adsorbate interactions, we have attempted to detect the platinum–carbon vibration of CO adsorbed on Pt(111). The international free-electron laser FELIX facility at the FOM Institute, Rijnhuizen, provided the required tunable far-infrared (19–23 μm) source for these experiments. Complementary results in the C–O stretch region (4.7–5.1 μm) were acquired at the University of Oxford with a conventional nanosecond laser system. While experimental and theoretical predictions of the $\nu_{\mathrm{Pt–CO}}$ intensity and line shape suggested that this mode could be detected, no SF resonance was observed. Some possible explanations for this finding are discussed along with the implications for the use of SFS for other systems.

1.1. Sum-frequency spectroscopy (SFS)

Sum-frequency generation (SFG) is a second-order nonlinear optical process whereby the interaction of two pulsed laser beams at an interface induces emission of light at the sum of the two frequencies [12]. In SFS, a pulsed fixed-frequency (typically visible) laser and a pulsed tunable infrared laser are used. A resonant enhancement of the SF signal occurs when the infrared frequency matches that of an SF-active vibrational mode of molecules at an interface. Scanning of the infrared beam over the desired frequency range produces a vibrational spectrum. Only interfacial molecules are SF-active within the electric dipole approximation. There is no direct contribution to the SF signal from any gas or liquid in contact with the surface, although absorption of the IR radiation by the bulk phase will reduce the intensity of the SF light emitted from the interface.

The intensity (I_{sum}) of the emitted SF light is proportional to the square of the modulus of the second-order susceptibility ($\chi^{(2)}$). $\chi^{(2)}$ can be expressed as the sum of a resonant component $\chi^{(2)}_{\mathrm{R}}$ (with frequency-dependent phase δ), arising from molecules at the interface, and a non-resonant component $\chi^{(2)}_{\mathrm{NR}}$ (with frequency-independent phase ε), arising from the substrate:

$$I_{\mathrm{sum}} \propto \left|\chi^{(2)}_{\mathrm{R}} + \chi^{(2)}_{\mathrm{NR}}\right|^2 = \left|\chi^{(2)}_{\mathrm{R}}\right|^2 + \left|\chi^{(2)}_{\mathrm{NR}}\right|^2 + 2\left|\chi^{(2)}_{\mathrm{R}}\right|\left|\chi^{(2)}_{\mathrm{NR}}\right|\cos(\varepsilon - \delta). \quad (1)$$

The resonant susceptibility, $\chi^{(2)}_{\mathrm{R}}$, is proportional to the product of the Raman and infrared transition dipole moments of the molecule. Thus, only molecular vibrations that are both Raman- and infrared-active will be SF-active. A corollary of this selection rule is that centrosymmetric molecules are SF-inactive unless interactions with the surface lower the symmetry. SFG is a coherent process and the angle at which light is emitted is set by conservation of momentum parallel to the surface.

1.2. Choice of CO/Pt(111)

For this study we sought a system for which at least a semi-quantitative estimation of the SF signal strength was possible. Among several metal–adsorbate systems considered, carbon monoxide adsorption on Pt(111) has several attractive features. From a purely experimental standpoint, it was necessary to choose a system that could be prepared easily, quickly, and reproducibly at FELIX. Ordered Pt(111) surfaces can be produced quite readily by the flame annealing approach of Clavelier [13]. This straightforward methodology has been used extensively by electrochemists to study CO adsorption on Pt(111) (for a review see [14]). The $\nu_{\mathrm{Pt–CO}}$ vibration has been studied by EELS (see, for example, [15]), SERS [11,16], infrared reflection–absorption spectroscopy (IRAS) [17–19] and IR emission [20]. The vibrational frequency of linearly bonded CO/Pt(111) varies from 460 to 478 cm^{-1} with temperature and coverage [17–19]. The FWHM has been found to be around 4–6 cm^{-1} at room temperature depending on the coverage [17–19]. The relatively high metal–adsorbate vibrational frequency and narrow band width would be helpful for distinguishing the Pt–CO resonance from the non-resonant background signal. The small non-resonant SF signal of platinum, compared with, for example, Au, Ag, or Cu, makes detection of weak resonant signals easier in general. Perhaps most importantly, the literature data [21–23] regarding the strength of the $\nu_{\mathrm{C–O}}$ SF resonance, along with available Raman [11,16] and infrared [17–19] data for this adsorption system, suggested that the $\nu_{\mathrm{Pt–CO}}$ stretch should be observable with SFS (see section 3.2).

2. Experimental

2.1. Flow reactor and CO/Pt(111) preparation

The Pt(111) single crystal (1 mm thick, 1 cm diameter, Goodfellow) was pretreated according to the general method established by Clavelier [13]. The crystal was annealed in a reducing hydrogen/oxygen flame for several seconds, cooled in dry N_2, transferred to the flow reactor,

and exposed to CO gas. This procedure resulted in reproducible CO monolayers on Pt(111), as judged from the SF spectrum of the ν_{C-O} stretch (*vide infra*). Carbon monoxide (99.9% pure), nitrogen (99.9% pure), helium (99.999% pure), hydrogen (99.995% pure) and oxygen (99.99% pure) were purchased from BOC or Hoek Loos B.V. and used without further purification. Gas flow rates, typically on the order of 100 $cm^3\,min^{-1}$, were measured with a bubble flow meter.

The reactor consisted of a stainless-steel vessel with a volume of ca. 50 cm^3 with a gas inlet/outlet and two windows. A rotating feedthrough attached to the sample mount allowed samples to be moved in and out of the laser beams during the experiment. The sample holder was heated resistively and its temperature measured with a K-type thermocouple. An antireflection-coated fused silica window was used for introduction of the visible beam into the flow reactor. A CaF_2 window was used for introduction of the IR beam during short wavelength (4.7–5.1 μm) SFS experiments, while a CsBr window was employed for long wavelength (19–23 μm) measurements. The angles of incidence used were approximately $\theta_{vis} = 50^\circ$ and $\theta_{IR} = 60^\circ$, although these values varied slightly with the wavelength of the IR.

2.2. The Oxford SF spectrometer

The SF spectrometer used to obtain spectra of the ν_{C-O} stretch under a range of flow-reactor conditions has been described in detail elsewhere [2a]. Briefly, the tunable IR beam (4.7–5.1 μm, 0.5 mJ/pulse, ca. 1 ns, 20 Hz) was produced by stimulated Raman scattering of a tunable dye laser beam (Spectron SL4000, LDS698 dye) in high-pressure hydrogen (26 bar). The visible beam (532 nm, 0.8 mJ/pulse, ca. 4 ns, 20 Hz) was provided by the frequency-doubled output of a Nd : YAG laser (Spectron). The green laser was reduced to a 2 mm diameter spot on the surface and the IR beam was gently focussed to fall within the green spot. The SF signal was detected with a Princeton Instruments liquid-N_2 cooled charge-coupled detector (CCD), with edge and band-pass filters to reject stray light. The IR bandwidth is sufficiently narrow (<0.2 cm^{-1}) to avoid any broadening of features; SF spectra were acquired point by point.

2.3. The FELIX SF spectrometer

The SF spectrometer used for the long wavelength (19–23 μm) experiments has been constructed as part of the user station for non-linear optical experiments at the FELIX free-electron laser at the FOM Institute, Rijnhuizen [9b]. The infrared beam supplied by FELIX arrives in $\sim$5 μs macropulses at a repetition rate of 5 Hz. Each macropulse contains a series of micropulses with a repetition rate of 1 GHz. The micropulse duration can be varied between 500 fs and 2 ps with an energy of approximately 10 μJ/pulse. The visible light (523 nm) from a frequency-doubled Nd : YLF laser system has a similar, but not identical, pulse structure: the macropulses ($\sim$5 μs, 5 Hz) contain 7 ps micropulses with a repetition rate of 250 MHz and an energy of 8 μJ/pulse. An rf system is used to synchronize the two beams at the sample surface on a ps timescale. As at Oxford, the laser beams were overlapped on the surface in a spot size of around 2 mm, with the IR focussed to fall within the green. The SF signal was detected with a Princeton Instruments liquid-N_2 cooled CCD and band-pass filters (Omega Optical, 510 nm (WL)) were used to reject stray light.

In contrast to the point-by-point spectral acquisition used at Oxford, we decided to take advantage of the natural broad bandwidth of the ultrashort FEL pulses. The emitted broadband SF signal is dispersed naturally on the CCD chip since the SF angle varies with IR frequency [9b,10]. The spectral resolution is determined by the CCD pixel size, diffraction, and dispersion. For the experiments described herein, the dispersion was 2.7 cm^{-1}/pixel from 19–23 μm, with a diffraction-limited resolution of ca. 7 cm^{-1}. The bandwidth of FELIX was ca. 15 cm^{-1} for these experiments and the FEL was typically scanned in small steps of $\sim$0.1 μm in order to cover a wider wavelength region. The SF spectrum from the sample was referenced to the non-resonant signal obtained from either a 200 nm Au film on Si or from the bare Pt(111) single crystal itself. The reactor, optics and laser beams were contained in a N_2-purged box to minimize the absorption of IR by water vapor.

3. Results and discussion

Experiments were first performed at Oxford in the 4.7–5.1 μm range to establish reproducible procedures for the production of high-quality CO/Pt(111) adlayers and to determine the effects of CO pressure and O_2 and H_2 treatments. Subsequent experiments were performed at FELIX in an attempt to detect the ν_{Pt-CO} stretch in the 19–23 μm region.

3.1. SFS of CO/Pt(111) in the 4.7–5.1 μm region

Figure 1 shows typical SF spectra for CO/Pt(111) under a range of gas-flow conditions at 298 K. A newly annealed Pt(111) crystal was first exposed to 1 atm of CO gas at 298 K for 5 min, after which the reactor was flushed out with pure N_2. A peak at 2078 cm^{-1} is observed from the CO monolayer in the presence of 1 atm of nitrogen (figure 1, bottom spectrum). This resonance arises from the ν_{C-O} stretching vibration and the frequency is indicative of CO adsorbed to terminal (or atop) sites. The intensity of this band was stable for at least 12 h under flowing nitrogen, although the frequency shifted gradually to lower wavenumbers. There was little change in either the intensity or frequency of the ν_{C-O} resonance upon exposure to gas flows containing CO partial pressures up to 0.1 atm (figure 1, middle spectrum). However, increasing the CO pressure to 1 atm (figure 1, top spectrum) resulted in a ca. 6 cm^{-1} increase in frequency and a significant decrease

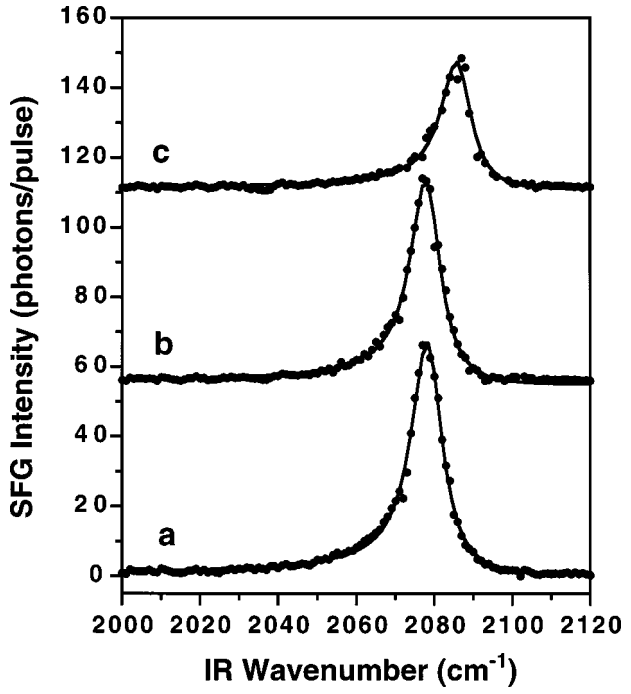

Figure 1. Sum-frequency spectra acquired in the 4.7–5.1 μm region from CO/Pt(111) at 298 K: (a) after treatment in 1 atm of CO for 5 min followed by displacement of CO with flowing N_2, (b) in 10% CO in N_2, and (c) in pure CO. The spectra have been offset for clarity and were obtained using 1 cm^{-1} frequency steps at 10 s/step. The solid lines are theoretical fits to the data for homogeneously broadened vibrations.

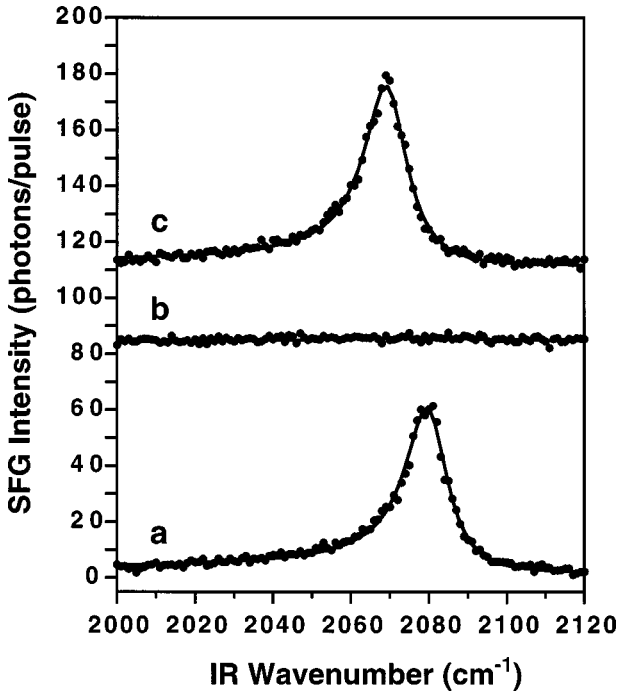

Figure 2. Sum-frequency spectra acquired in the 4.7–5.1 μm region from CO/Pt(111) at 298 K: (a) after treatment in 1 atm of CO for 5 min followed by displacement of CO with flowing N_2, (b) after an O_2/H_2 heating treatment (see text for details), and (c) in flowing N_2 after re-exposure to 1 atm of CO. The spectra have been offset for clarity and were obtained using 1 cm^{-1} frequency steps at 10 s/step. The solid lines are theoretical fits to the data for homogeneously broadened vibrations.

in intensity. Nevertheless, the $\nu_{C–O}$ signal intensity was still readily detectable and the bandwidth not substantially changed. No concerted attempt was made to detect the $\nu_{C–O}$ stretch of CO adsorbed at two-fold bridging sites, which is typically found at around 1850 cm^{-1} [23].

Our results are qualitatively similar to those obtained previously by SFS for this system [22,23]. A notable difference is that the frequency of the $\nu_{C–O}$ vibration in our experiments is 12–20 cm^{-1} lower than in previous UHV studies on Pt(111) crystals prepared by Ar^+ sputtering and high-temperature annealing [3,20,21]. A sharp C–O stretch persists to higher pressures than in the previous work of Somorjai. These differences serve to underline the sensitivity of the adsorption characteristics of CO to the density of defects and impurity levels on the Pt(111) surface.

The most satisfactory reference for the Pt/CO monolayer in the far-IR is the non-resonant signal from the bare Pt(111) surface itself. An oxidation/reduction procedure was therefore employed to remove CO from the Pt(111) surface. The CO/Pt(111) surface (figure 2, bottom spectrum) was first heated in 1 atm of O_2 to 373 K for 5 min, and then cooled to 298 K. The surface oxide was then reduced with 1 atm of H_2 at 373 K for 5 min. The sample was cooled to 298 K, and the reactor flushed with N_2. The disappearance of the $\nu_{C–O}$ feature (figure 2, middle spectrum) reveals that the adsorbed CO is completely removed by this treatment. Moreover, the intensity and profile of the resulting non-resonant SF signal is largely unchanged. Exposing this surface to 1 atm CO at 298 K followed by flowing N_2 (figure 2, top spectrum) resulted in a return of the $\nu_{C–O}$ feature to its previous intensity. The 10 cm^{-1} redshift in frequency and a slight increase in bandwidth are likely to be a result of changes in the Pt(111) surface structure caused by the O_2/H_2 treatment.

3.2. Estimation of expected $\nu_{Pt–CO}$ signal strength

To predict the intensity of the $\nu_{Pt–CO}$ mode in an SF spectrum we need estimate the relative magnitudes of $\chi_R^{(2)}$ and $\chi_{NR}^{(2)}$. The resonant susceptibility, $\chi_R^{(2)}$, is directly proportional to the product of the dynamic dipole moment (μ) and the Raman tensor (α). Malik and Trenary [18] report that the $\nu_{Pt–CO}$ infrared absorbance is ca. 40 times weaker than that for the $\nu_{C–O}$ stretch, while Hoge et al. [17] estimate the difference to be around 70. The integrated absorbance scales as $\omega\mu^2$, where ω is the vibrational frequency. If we ignore differences in linewidth (an approximation that does not affect our final estimate of SF signal strength), μ for the $\nu_{Pt–CO}$ stretch is 3–4 times smaller than for the strong $\nu_{C–O}$ vibration. Normal Raman spectra do not exist for Pt(111)/CO, however, SERS data do exist for thin polycrystalline Pt films deposited on roughened gold [16a]. While it is difficult to compare band intensities quantitatively from available SERS studies, the data suggests that the intensity of the $\nu_{Pt–CO}$ stretch is roughly three-fold weaker than for the $\nu_{C–O}$ mode. After allowing for the ω^4 dependence of Raman scattering, we estimate that α for the $\nu_{Pt–CO}$ mode is

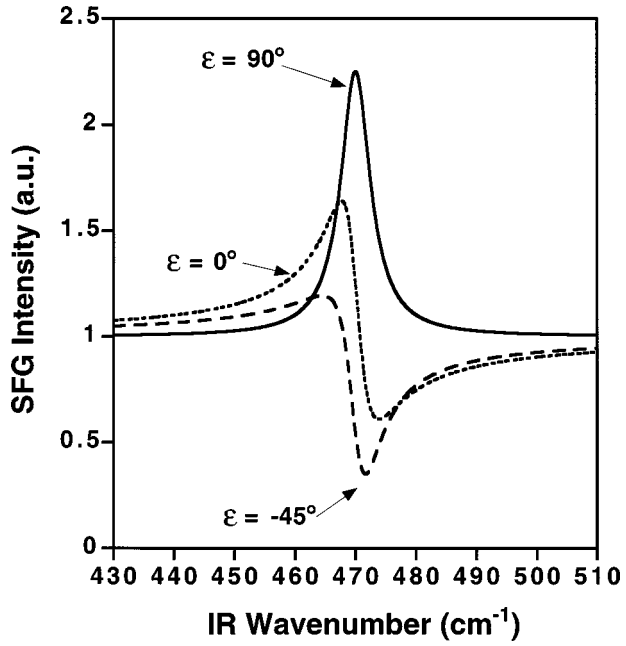

Figure 3. Theoretical lineshapes calculated for the $\nu_{\mathrm{Pt–CO}}$ stretch using equation (1), with the phase of $\chi^{(2)}_{\mathrm{NR}}$ equal to 90° (solid line), 0° (small dashed line), and −45° (large dashed line), a vibrational frequency of 470 cm^{-1} and a Lorentzian half-width of 3 cm^{-1}. See text for details regarding the estimation of the strength of $\chi^{(2)}_{\mathrm{R}}$ for the $\nu_{\mathrm{Pt–CO}}$ mode.

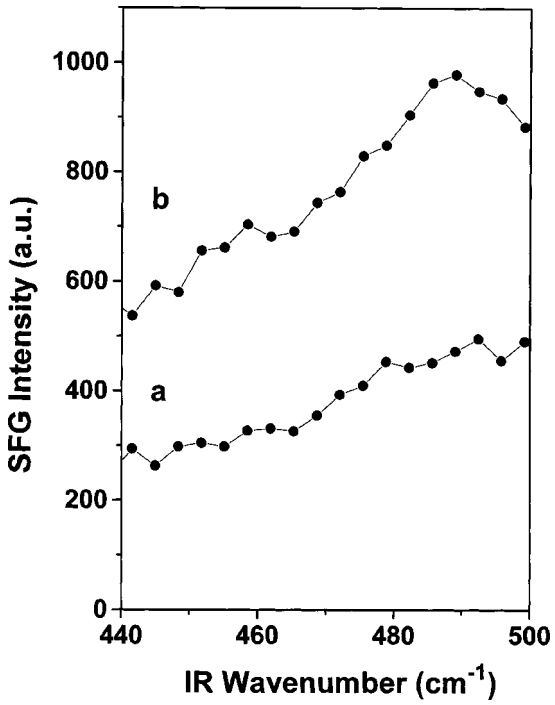

Figure 4. Sum-frequency signal acquired in the 19–23 μm region from Pt(111) at 298 K in the presence of (a) 10% CO in flowing He and (b) in flowing He after an O_2/H_2 heating treatment (see text for details). The spectra have been offset for clarity and were obtained with 0.1 μm wavelength steps at 15 s/step.

approximately one half that of the $\nu_{\mathrm{C–O}}$ stretch. We therefore estimate that $\chi^{(2)}_{\mathrm{R}}$ for the $\nu_{\mathrm{Pt–CO}}$ mode should be 6–8 times weaker than for the $\nu_{\mathrm{C–O}}$ vibration.

From the dependence of the overall SF signal on the second-order susceptibilities (equation (1)), an estimate of the signal strength for the $\nu_{\mathrm{Pt–CO}}$ feature can be made. In the present study, a ratio of $|\chi^{(2)}_{\mathrm{R}}/\chi^{(2)}_{\mathrm{NR}}| \approx 4$ was calculated at the peak of the $\nu_{\mathrm{C–O}}$ vibration in the presence of 0.1 atm CO at 298 K (figure 1, middle spectrum). A similar value of $|\chi^{(2)}_{\mathrm{R}}/\chi^{(2)}_{\mathrm{NR}}| \approx 3$ has been reported by Harle et al. [22] at the peak of the $\nu_{\mathrm{C–O}}$ stretch at 2088 cm^{-1} on sputtered Pt(111). Assuming that $\chi^{(2)}_{\mathrm{NR}}$ is independent of infrared frequency, we would predict that $|\chi^{(2)}_{\mathrm{R}}/\chi^{(2)}_{\mathrm{NR}}| \approx 0.5$ on the peak of the $\nu_{\mathrm{Pt–CO}}$ stretch. Using this ratio along with equation (1), we can calculate theoretical line shapes for the $\nu_{\mathrm{Pt–CO}}$ mode. The phase of the non-resonant background is *a priori* unknown, so in figure 3 we show calculated SF spectra for $\varepsilon = 90°$ (solid line), 0° (small dashed line), and $-45°$ (large dashed line), revealing a range of possible line shapes. Even for the least favorable (and most likely) case where the SF feature has a derivative shape ($\varepsilon = 0°$), the resonance should clearly be visible above the anticipated noise level.

3.3. SFS of CO/Pt(111) in the 19–23 μm region

The samples at FELIX were prepared according to procedures identical to those used at Oxford. Although the $\nu_{\mathrm{C–O}}$ stretch lies just outside the usable wavelength range of FELIX, and, therefore, could not be used to check the quality of the monolayers, we are confident that well-formed monolayers were produced. The far-infrared experiments were performed with a pressure of 0.1 atm of CO in the reactor, since the quality of the CO/Pt(111) adlayer remains unchanged under these conditions (cf. figure 1). The overpressure of CO also provides a source for CO to readsorb on the surface in the event of laser-induced desorption (*vide infra*). Both gold and Pt(111) reference signals were acquired in addition to the sample spectrum. Figure 4 shows a representative example of the SF signal (between 19 and 23 μm) obtained from both a CO-covered (top) and bare (bottom) Pt(111) surface. The raw signal arising from CO/Pt(111) reveals no apparent vibrational resonance. Furthermore, using the non-resonant signal from bare Pt(111) as a reference to account for changes in infrared power with wavelength did not produce any vibrational features; using the gold reference (not shown) also yielded no spectral feature.

One possible explanation for the absence of the $\nu_{\mathrm{Pt–CO}}$ resonance is that the CO adlayer might desorb from the Pt(111) surface as a result of irradiation by the two laser beams. Even with 0.1 atm of CO in the gas phase during these measurements, only 3% of a monolayer of CO would readsorb in 1 ns on a bare Pt(111) surface (assuming a sticking probability of unity). Given the high repetition rates of these picosecond-length laser pulses, there might not be enough time to replenish any CO that might desorb with each pulse. Thus, if each micropulse induced even a small amount of CO desorption, the coverage of CO might fall rapidly to a fraction of a monolayer. Such a circumstance would, based on our calculations of the expected

band intensity (*vide supra*), make observation of the $\nu_{\mathrm{Pt–CO}}$ stretch impossible.

Two different laser-induced desorption mechanisms were considered. The first possibility is that photo-induced CO desorption occurs as the infrared laser is scanned through the $\nu_{\mathrm{Pt–CO}}$ vibrational frequency. Based on the experimental IRAS results of Malik and Trenary [18] we estimate that each adsorbed CO molecule absorbs around 0.01 photons/micropulse. Such a low photon flux could not cause multiphoton dissociation of the Pt–CO bond. The second possible route to CO desorption would be laser-induced heating of the surface above the desorption temperature of this molecule. From published optical constants of Pt [24], we estimate that the maximum increase in surface temperature arising from the partial absorption of the green and the infrared micropulses is ca. 30 K/micropulse (for a discussion of laser-induced heating of metal surfaces see [25]). The temperature drops rapidly between micropulses due to diffusion into the bulk metal. A similar temperature rise is also predicted if one considers the average power within a macropulse rather than a micropulse. Based on published values for CO desorption kinetics from Pt(111) [26], a negligible amount of CO would desorb during the length of time (a few ps) that the surface temperature is elevated. Thus, we can rule out CO desorption as a reason for the absence of the $\nu_{\mathrm{Pt–CO}}$ vibrational resonance.

A more likely explanation for the discrepancy between the predicted and measured intensities of the Pt–CO mode may rest in our estimation of the Raman tensor, which was based on SERS measurements [16]. An implicit assumption was made that the level of enhancement for both the ν_{CO} and $\nu_{\mathrm{Pt–CO}}$ stretches is similar. If the *actual* value of α for the $\nu_{\mathrm{Pt–CO}}$ stretch is much smaller than that for the intramolecular vibration, the true value of $|\chi^{(2)}_{\mathrm{R}}/\chi^{(2)}_{\mathrm{NR}}|$ for the $\nu_{\mathrm{Pt–CO}}$ mode would be much smaller than estimated. It is apparent from the theoretical spectra in figure 3 that a significant drop in resonant signal intensity would greatly diminish the chances of detecting this vibration. Indeed, based on the signal to noise ratio evident from figure 4 it would be difficult to discern a resonance over the nonresonant background signal if $|\chi^{(2)}_{\mathrm{R}}/\chi^{(2)}_{\mathrm{NR}}| \leqslant 0.1$.

4. Concluding remarks

While SFS continues to make an impact in the study of heterogeneous catalytic (and other) interfaces, the failure to detect the $\nu_{\mathrm{Pt–CO}}$ mode of CO/Pt(111) does not bode well for use of this approach to examine low-frequency metal–adsorbate vibrations in the future. While SF studies of other adsorption systems (e.g., NO/Ir(111), Cl/Au(111)) might be attempted, the CO/Pt(111) system was arguably among the most favorable in terms of chances for success. One of the main problems in initiating far-infrared SF studies of this sort remains the lack of even semi-quantitative IR and Raman spectroscopic information that allows reliable estimation of the expected metal–adsorbate resonance intensities. This situation is compounded by the high cost and time constraints imposed by a free-electron laser facility. A major technological advance such as the development of a benchtop laser system capable of generating the necessary high-power far-infrared light may change this situation in the future by allowing more extensive investigations to be pursued.

Acknowledgement

We gratefully acknowledge the financial support of the EPSRC, the Technology Foundation (STW) and the Stichting voor Fundamenteel Onderzoek der Materie (FOM). We appreciate the highly skilful assistance of the FELIX staff, in particular Dr. Guido Knippels and Dr. Lex van der Meer. This work was supported in part under the TMR programme of the European Community. We thank Dr. Eric Eliel (Leiden) for advice and for the loan of equipment. CTW acknowledges the receipt of an NSF-NATO Post Doctoral Fellowship and YY thanks the K.C. Wong Education Foundation for support.

References

[1] D.W. Goodman, J. Phys. Chem. 100 (1996) 13090.
[2] (a) C.D. Bain, J. Chem. Soc. Faraday Trans. 91 (1995) 1281;
(b) A. Tadjeddine and A. Peremans, in: *Advances in Spectroscopy*, Vol. 26, eds. R.J.H. Clark and R.E. Hester (Wiley, Chichester, 1998) ch. 4.
[3] X. Su, J. Jensen, M.X. Yang, M.B. Salmeron, Y.R. Shen and G.A. Somorjai, Faraday Discuss. 105 (1996) 263.
[4] (a) P.S. Cremer, X. Su, Y.R. Shen and G.A. Somorjai, J. Am. Chem. Soc. 118 (1996) 2942;
(b) P.S. Cremer, X. Su, Y.R. Shen and G.A. Somorjai, J. Chem. Soc. Faraday Trans. 92 (1996) 4717.
[5] X. Su, Y.R. Shen and G.A. Somorjai, Chem. Phys. Lett. 280 (1997) 302.
[6] A. Bandara, S. Dobashi, J. Kubota, K. Onda, A. Wada, K. Domen, C. Hirose and S.S. Kano, Surf. Sci. 387 (1997) 312.
[7] (a) K. Domen, N. Akamatsu, H. Yamamoto, A. Wada and C. Hirose, Surf. Sci. 283 (1993) 468;
(b) K. Domen, H. Yamamoto, N. Watanabe, A. Wada and C. Hirose, Appl. Phys. A 60 (1995) 131.
[8] (a) N. Akamatsu, K. Domen and C. Hirose, J. Phys. Chem. 97 (1993) 10070;
(b) P. Guyot-Sionnest, J.H. Hunt and Y.R. Shen, Phys. Rev. Lett. 59 (1987) 1597;
(c) D. Zhang, J. Gutow and K.B. Eisenthal, J. Phys. Chem. 98 (1994) 13729;
(d) P. Guyot-Sionnest, J. Electron Spectrosc. Relat. Phenom. 64 (1993) 1;
(e) P. Rabinowitz, B.N. Perry and N.J. Levinos, IEEE J. Quantum Electron 22 (1986) 797;
(f) A.L. Harris and N.J. Levinos, Appl. Opt. 26 (1987) 3996.
[9] (a) CLIO in Orsay: A. Tadjeddine, A. Peremans and P. Guyot-Sionnest, Surf. Sci. 335 (1995) 210;
(b) FELIX in Rijnhuizen: W.M. van der Ham, Q.H.F. Vrehen and E.R. Eliel, Opt. Lett. 21 (1996) 1448.
[10] R. Braun, B.D. Casson, C.D. Bain, E.W.M. van der Ham, Q.H.F. Vrehen, E.R. Eliel, A.M. Briggs and P.B. Davies, J. Chem. Phys. 110 (1999) 4634.
[11] (a) C.T. Williams, A.A. Tolia, H.-Y.H. Chan, C.G. Takoudis and M.J. Weaver, J. Catal. 163 (1996) 63;

(b) C.T. Williams, C.G. Takoudis and M.J. Weaver, J. Phys. Chem. B 102 (1998) 406.
[12] Y.R. Shen, *The Principles of Non-Linear Optics* (Wiley, New York, 1984).
[13] J. Clavelier, J. Electroanal. Chem. 107 (1980) 211.
[14] M.J. Weaver, J. Phys. Chem. 100 (1996) 13079.
[15] A.M. Baro and H. Ibach, J. Chem. Phys. 71 (1979) 4812.
[16] (a) S. Zou and M.J. Weaver, J. Phys. Chem. 100 (1996) 4237;
(b) Z.Q. Tian, B. Ren and B.W. Mao, J. Phys. Chem. B 101 (1997) 1338.
[17] D. Hoge, M. Tushaus, E. Schweizer and A.M. Bradshaw, Chem. Phys. Lett. 151 (1988) 230.
[18] I.J. Malik and M. Trenary, Surf. Sci. 214 (1989) L237.
[19] (a) R. Ryberg, Phys. Rev. B 40 (1989) 8567;
(b) B.N.J. Persson and R. Ryberg, Phys. Rev. B 40 (1989) 10273;
(c) R. Ryberg, J. Electron Spectrosc. Relat. Phenom. 54/55 (1990) 65;
(d) R. Ryberg, Phys. Rev. B 44 (1991) 13160.
[20] R.G. Tobin and P.L. Richards, Surf. Sci. 179 (1987) 387.
[21] (a) P. Guyot-Sionnest and A. Tadjeddine, Chem. Phys. Lett. 172 (1990) 341;
(b) A. Peremans and A. Tadjeddine, Chem. Phys. Lett. 220 (1994) 481;
(c) A. Peremans, A. Tadjeddine and P. Guyot-Sionnest, Chem. Phys. Lett. 247 (1995) 243.
[22] H. Harle, K. Mendel, U. Metka, J.-R. Volpp, L. Willms and J. Wolfrum, Chem. Phys. Lett. 279 (1997) 275.
[23] X. Su, P.S. Cremer, Y.R. Shen and G.A. Somorjai, Phys. Rev. Lett. 77 (1996) 3858.
[24] D.R. Lide and H.P.R. Frederikse, eds., *CRC Handbook of Chemistry and Physics*, 74th Ed. (CRC Press, London, 1993) pp. 12–135.
[25] J.H. Bechtel, J. Appl. Phys. 46 (1975) 1585.
[26] L.P. Ford, H.L. Nigg, P. Blowers and R.I. Masel, J. Catal. 179 (1998) 163.